INFLUENCE OF BLAST LOAD MODELLING ON DYNAMIC RESPONSE OF STRUCTURES

[1]MICHAŁ LIDNER, [2]ZBIGNIEW SZCZESNIAK

Faculty of Civil Engineering and Geodesy, Military University of Technology, Poland
Email: michal.lidner@wat.edu.pl, zbigniew.szcześniak@wat.edu.pl

Abstract- The paper presents a new own method of modeling of the air shock wave generation and propagation. Conception of the method refers to the idea of Finite Volume Method and takes into account energy losses with respect to an adiabatic process rule. A charge explosion in the air was analyzed. A congeneric simulation was done considering spatial propagation of post-explosion gases and air shock wave and also dynamic response of isolated structural element.

Index Terms- Adiabatic Process Rule, Blast Load, Dynamic Response, Finite Volume Method

I. INTRODUCTION

When considering human activity nowadays one can meet the blast load overpressure caused by different actions. From the point of view of people and building security one of the main destroying factors is the air shock wave. Rational estimating of blast load results should be preceded with knowledge of complex wave field distribution in time and space. As a result one can estimate the blast load distribution in time and space applied to structural elements. In technical conditions, the values of blast load are estimating using the empirical functions of overpressure distribution in time (Δp(t)) [1]-[7]. The Δp(t) functions are monotonic and are the approximation of reality. Additionally, distributions of these functions are often linearized due to simplifying of estimating the blast reaction of elements.

The ability to estimate blast load overpressure properly plays an important role in safety design of covers, shelters and also buildings. This issue is much more important when the space affected by explosion is inhibited by several factors. In such situations scientific papers consider often simplified conception of blast load and its reflection. When considering mentioned references authors think that the more development of air shock wave propagation and blast load distribution in time is needed.

II. GENERAL CHARACTERISTIC OF BLAST LOAD MODELING

A. Shock Wave Region

The unknown Δp(t) function reflects the thermodynamic state in each point of disturbed gaseous medium, and also reflects the influence of the boundary conditions. The most advanced models available nowadays for Computational Fluid Dynamics are based on Finite Volume formulations, in which the governing equations for the fluid domain (equations for a compressible inviscid fluid, expressing the conservation of mass, momentum and energy) are formulated and solved in conservative form (see ref. [8]). Thus conservation of mass, momentum and energy in gaseous medium about the density equal to ρ can be written as follows:

$$\frac{\partial}{\partial t}\iiint_V \rho dV + \iint_S \rho v_n dS = 0, \tag{1}$$

$$\frac{d}{dt}\left(\iiint_V \rho \vec{v}\, dV\right) = \iint_S p_n dS + \iiint_V \rho \vec{F}_m\, dV, \tag{2}$$

$$\frac{d}{dt}\left[\iiint_V \rho\left(c_v T + \frac{v^2}{2}\right)dV\right] = \iint_S p_n v_n dS + \iiint_V \rho \vec{F}_m \vec{v}\, dV + \iint_S \dot{q}_n\, dS + \iiint_V \dot{q}_m\, \rho dV, \tag{3}$$

where: t – time, S – surface area of the considered finite volume about volume equal to V, v_n – flow rate of the gaseous medium by the surface S, $\vec{v}$ – velocity vector consisting of components [u, v, w] in each of the three orthogonal directions, p_n – pressure by the surface dS, $\vec{F}_m$ – unit vector of internal forces, c_v – specific heat of the gaseous medium at constant volume, T – temperature of gaseous medium, $\dot{q}_n$ – surface density of the heat flux, $\dot{q}_m$ – heat flux density related to the unit mass of the gas.

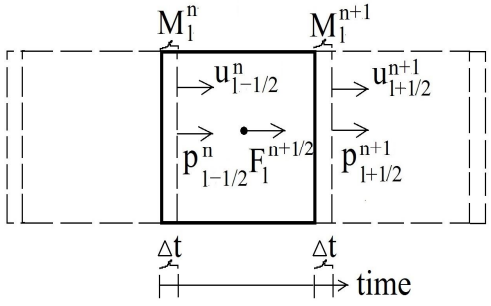


Fig. 1. Diagram of gas flow inside considered finite volume

The system of equations (1) to (3) expresses the gaseous medium flow in the free field region. Solving this system of equations can help present evolution of blast load parameters in time and free-field space and was made using own numerical algorithm (see ref. [9], [10]). Graphical interpretation is presented in Fig. 1. The considered volume of gaseous medium is outlined by thick lines and the adjacent volumes by dotted lines. It is assumed that the two parallel sides are being displaced with velocities $U^n_{l-1/2}$ and $U^n_{l+1/2}$ due to changes in energy. This results in displacement of the mass (M) of gaseous medium to a finite volume, which is highlighted by thick line, and hence the change of density and mass of this volume. Weight increase is associated with a pressure change (p). Consequently, there is also a change in energy. Next, a loop is performed over all finite volumes for the following time steps in order to compute the internal forces. Integration of mentioned equations is made using explicit difference scheme.

The system of equations must be supplemented by the boundary conditions at the interface of building compartments with adjacent finite volumes and at the point of detonation of condensed explosive. When assuming boundary conditions one can simulate the inhibition of gaseous flux by the building compartments. The assumption of the compartment velocity equal to zero (boundary condition) in case of high mass of compartments (concrete, RC) is reasonable, because the blast loading is completed before the compartment deformation started [11]. When considering light compartments (made of steel or glass) a suitable coupling strategy must be chosen. One of the best is the strategy based upon suitable kinematic constraints on the velocities of the fluid and of the structure along the fluid-structure interface. In the point, when the shock wave region starts, some boundary condition should be known. These are the particle velocity $U_{1/2}{}^1$, the shock wave pressure $p_{1/2}{}^1$, the density of post-explosion gases $\rho_1{}^1$ and the temperature of post-explosion gases (see ref. [12]-[14]).

B. Region of Post-Explosion Gases

In case of spherical charge gasses has the shape of a sphere, and in case of cubical charge the shape of an octahedron [15]. In case of a spherical charge, post-explosion gases propagate till 7th time step (2 x 6.5 = 13 – the medium between 10 and 15). Then the density of post-explosion gases is equal to the air density in 7th time step and till this point the shock wave begins to propagate. In case of a cubical charge the region of post-explosion gases finishes in 9th time step. This difference is due to bigger volume of a sphere than an octahedron entered into this sphere. Discrete regions of post-explosion gases in case of spherical charge (till 7th time step) and cubical charge (till 9th time step) are presented in Fig. 2. Boundary conditions in air shock wave region should be equal to the results of calculating parameters in the region of post-explosion gases.

III. COMPARING NUMERICAL RESULTS WITH LITERATURE REPORTS

This paragraph contains checking of correctness of modeling presented in section II. The verification involved comparing calculated blast overpressure distributions in time with measured distributions [16]. Detonations of point charges inside steel and concrete composite structure were analyzed. To validate correctness of three-dimensional solution, blast pressure distribution from a detonation of 1 kg TNT charge in the center point of a vented room was examined [8]. The room was a composite steel and concrete structure of a horizontal square projection with a side of 2.9 m and height 2.7 m (internal dimensions) with a hole in the roof of 1.20 m in diameter (Fig. 3). Authors assumed that elements of the structure and entrances were rigid. 9 pressure gauges were installed on one of the walls (G1 to G9).

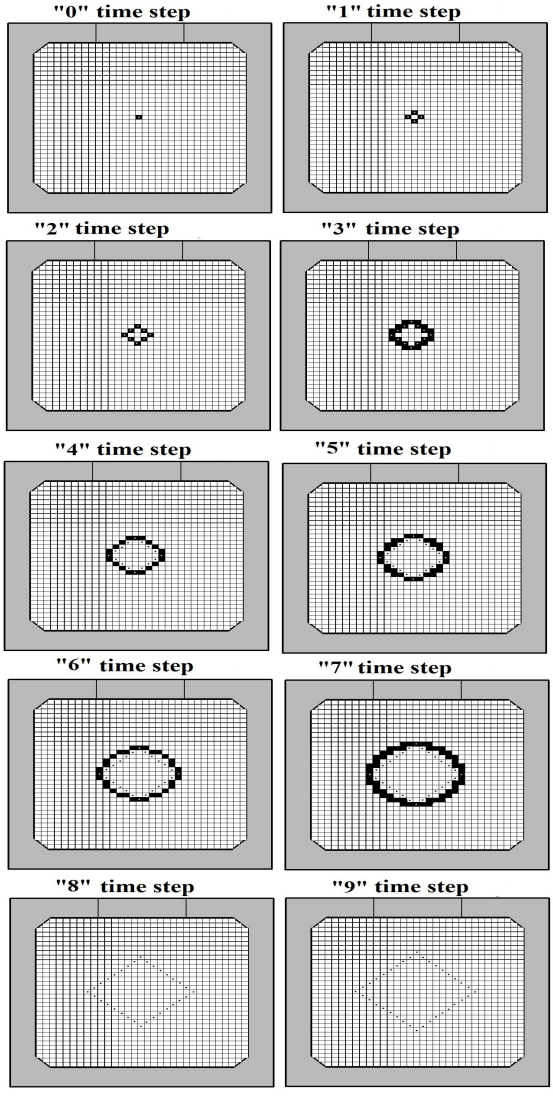


Fig. 2. Discrete spheres(drawn using squares) and octahedrons(drawn using dots) in the following time steps.

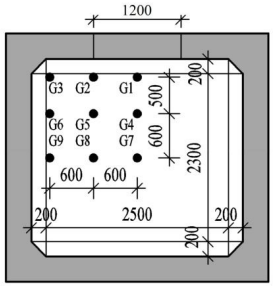


Fig. 3. Test stand scheme

A numerical model was obtained in this case through applying the 3D model of the air shock wave propagation presented in [9], [10]. Internal space of the considered room was divided by cubical finite volumes. Dimension of this volume $\Delta x=\Delta y=\Delta z$ is equal to 0.085 m. The mass velocity of the volumes located next to room`s compartments was assumed for zero in each time step. The mass velocity of side volumes, located next to free-field or in openings, can be of any value. The time step value was assumed for $\Delta t=0.012$ *ms.*

The cell size should not be bigger than the charge dimension. The compartment velocity is equal to zero because of assuming rigid compartments. The time step value (Δt) is equal to Δx/7000. This is the time to reach the distance of first cell by the shock wave (the TNT detonation velocity – 7000 m/s). Initial conditions are: the mass velocity $U_{1/2}{}^{1}$ equal to 690 m/s and the detonation pressure $p_{1/2}{}^{1}$ equal to 6.7 MPa [10].

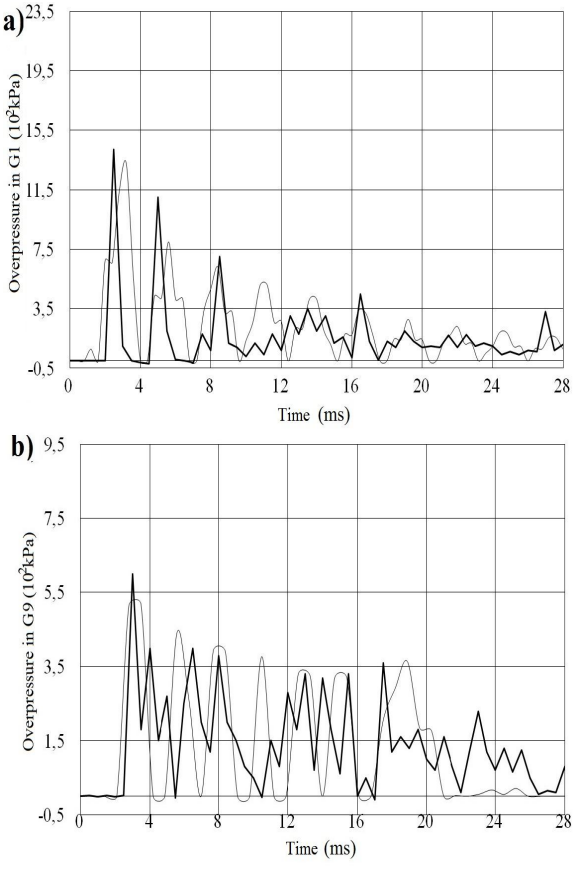


Fig. 4. Overpressure distribution in time: a) in location of gauge G1, b) in location of gauge G9 (thick line – research results; thin line – numerical results).

Fig. 4 presents graphs with an overpressure versus time in gauges G1, and G6. As can be seen, numerical results reflect well the time to reach the shock wave and the duration of the shock wave. It can also be observed that when the overpressure obtained in the tests increases, the overpressure obtained numerically also increases. The same applies to the overpressure decrease. The values of maximum overpressures and impulses (area under the overpressure graph) obtained numerically and those from literature reports are similar.

IV. DYNAMIC RESPONSE OF STRUCTURAL ELEMENT

Present paragraph contains analyses of dynamic response of a structure which was blast loaded. The literature reports provide many different blast load distribution models. This paper considers the exponential and the triangular models [17] and also the model proposed in this article, called later as realistic. Simplified methods of blast load estimation inside vented or unvented room rely mainly on using empirical equations [17].

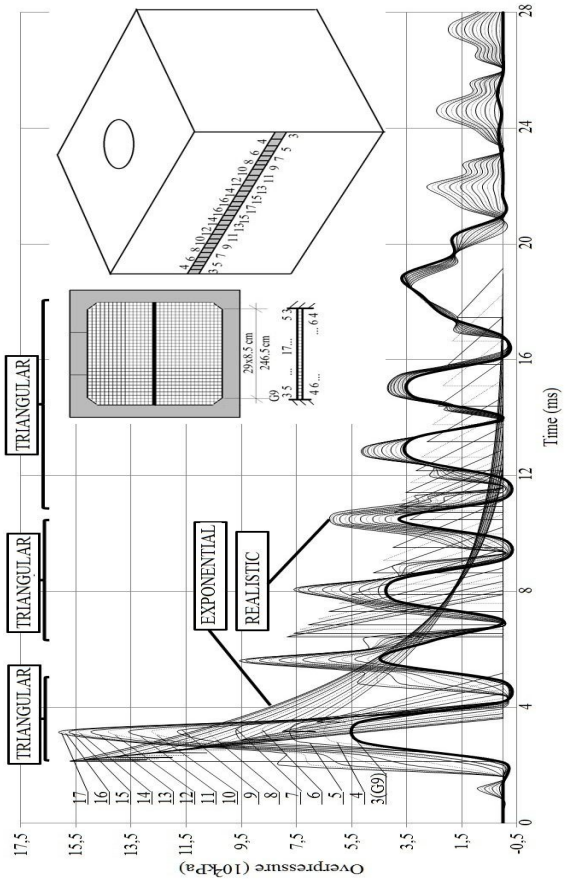


Fig. 5. a) overpressure distribution in time in points 3÷17 for exponential, triangular and realistic model; b) room cross-section i c) axonometric projection of room with hatched isolated beam and points 3÷17

Assessment of previously mentioned blast load models was made using comparison of deflection change in time when considering the isolated structural element. Nowadays this is common approach because within maximum peak deflection one can easily find the residua deflection. Deflection analysis was prepared using overpressure distribution in time inside considered room.

As a result of presented modeling air shock wave parameters can be obtained in each finite volume inside considered room (fig. 5). Figure 5 presents isolated part of the wall which was divided by 33 cells and the overpressure distributions (for three kinds of models) are presented for each cell, strictly for 15 cells in locations 3÷17 because of symmetry (fig. 5a).

In second step, dynamic response of isolated structural beam element was made. The location of the beam and its scheme are presented in fig. 5b and 5c, respectively. It was assumed that the supports are fixed, length is equal to 2.465 m, width of cross-section is equal to 8.5 cm, height 19 cm (including: steel plate, thickness 1 cm; concrete, thickness 17 cm; steel plate, thickness 1 cm), f_{yk}=235 MPa, E_S=210 GPa, f_{ck}=25MPa, E_c=31 GPa. The damping also was taken into consideration, characterized using modified friction damper equal to 0.25. Free vibration period is equal to 0.0097 s.

The dynamic analyses were made using Finite Difference Scheme and integration of dynamic differential equations of Bernoulli beam. The model of a beam is characterized using system of discrete mass located along longitudinal beam axis in nodes offset equal to Δx.

The equation of motion in i-th node can be written as:

$$P_i^n + Q_i^n - Q_{i-1}^n - B_i^n - S_{c,i}^n = 0, \qquad (4)$$

where: P_i^n – force determined by multiplying the overpressure value by beam width and Δx value, Q_i^n, Q_{i-1}^n – transverse forces, $B_i^n = \Delta m \ddot{w}$ – inertia force, $S_{c,i}^n = c\dot{w}$ – damping force, Δm – discrete mass, w – node deflection, c – friction damper.

Equation of motion were integrated using Finite Difference Scheme in time. The curvature in i-th node can be calculated as:

$$k_i^n = \left(w_{i-1}^n - 2w_i^n + w_{i+1}^n\right)/\Delta x^2. \qquad (5)$$

The moment-curvature physical law was used so the bending moment can be written as:

$$M_i^n = k_i^n B_c, \qquad (6)$$

where B_c – bending stiffness of beam cross-section.

Transverse force can be calculated using condition of bending moments balance against i-th node:

$$Q_i^n = \left(M_{i+1}^n - M_i^n\right)/\Delta x. \qquad (7)$$

Graphs of deflections change in time are presented in Fig. 6. Beam vibrations with considering damping are presented using thick lines and vibrations without considering damping are presented using dotted lines. Maximum deflections influenced realistic model of overpressure are about 30% less than deflections influenced exponential model, however the impulse applied in case of realistic overpressure is 200% bigger than in case of exponential overpressure. Maximum deflections influenced triangular model of overpressure are about 50% less than deflections influenced realistic model, however the impulse applied in case of triangular overpressure is 400% less than in case of realistic overpressure. This is a result of applying further overpressure impulses to the beam when it comes back to the location before deformation. This provides velocity reduction of deformed beam.

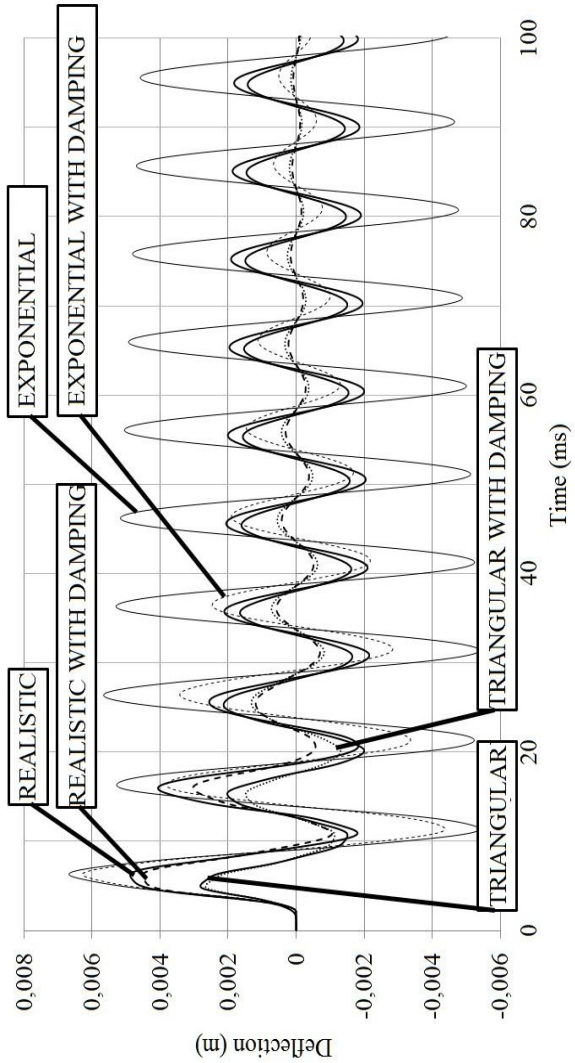


Fig. 6. Change of deflection in time in dependents from blast load distribution model

This work was supported by grant RMN No 800/2016 funded by Faculty of Civil Engineering and Geodesy in Military University of Technology.

REFERENCES

[1] A. Zare, M. Janghorban, "Shock factor investigation in a 3-D finite element model under shock loading," *Lat. Am. J. Solids Struct.*, vol. 10, pp. 941-952, January 2013.

[2] Z. M. Jaini, Y. T. Feng, D. R. J. Owen, S. N. Mokhtar, "Fracture Failure of Reinforced Concrete Slabs Subjected to Blast Loading Using the Combined Finite-Discrete Element Method," *Lat. Am. J. Solids Struct.*, vol. 13, pp. 1086-1106, February 2016.

[3] H. R. Tavakoli, F. Kiakojouri, "Numerical dynamic analysis of stiffened plates under blast loading," *Lat. Am. J. Solids Struct.*, vol. 11, pp. 185-199, January 2014.

[4] J. Siwiński, A. Stolarski, "Analysis of the external explosion action on the building barriers," *Bulletin MUT*, vol. 64, no. 2, pp. 173-196, June 2015. (in Polish)

[5] M. Lidner, "Numerical Calculation of a Blast Load on the Example of a Slab and Wall Structure of any Geometry (Published Conference Proceedings style)," in *Proc. 5th Intl Worksh. Performance, Protection & Strengthening of Structures Under Extreme Loading*, East Lansing, 2015, pp. 563–570.

[6] M. Lidner, Z. Szcześniak, "Numerical Calculation of a Blast Load," *Logistyka*, no. 4, pp. 9397-9403, September 2015. (in Polish)

[7] M. Lidner, Z. Szcześniak, "Simplified Numerical Modelling of a Blast Load Impact," *Appl. Mech. Mater.*, vol. 797, pp. 131-136, November 2015.

[8] F. Casadei, N. Leconte, "Coupling finite elements and finite volumes by Lagrange multipliers for explicite dynamic fluid-structure interaction," *Int. J. Numer. Methods Eng.*, vol. 86, no. 1, pp. 1-17, April 2011.

[9] M. Lidner, Z. Szcześniak, "Numerical Analysis of Blast Load from Explosive Materials Using Finite Volume Method," *Key Eng. Mat.*, vol. 723, pp. 789-794, January 2017.

[10] M. Lidner, Z. Szcześniak, "Blast load estimation using Finite Volume Method and linear heat transfer," *MATEC Web Conf.*, vol. 86, 01027, December 2016.

[11] V. T. Nguyen, B. A. Gatzhammer, "Fluid structure interactions partitioned approach for simulations of explosive impacts on deformable structures," *Int. J. Impact Eng.*, vol. 80, pp. 65-75, February 2015.

[12] L. Mazurkiewicz, J. Malachowski, P. Baranowski, "Blast loading influence on load carrying capacity of I-column," *Eng. Struct.*, vol. 104, pp. 107-115, December 2015.

[13] A. Erdik, S. A. Kilic, N. Kilic, S. Bedir, "Numerical simulation of armored vehicles subjected to undercarriage landmine blast," *Shock Waves*, vol. 26, pp. 449-464, May 2015.

[14] B. Yan, F. Liu, D. Y. Song, Z. Jiang, "Numerical study on damage mechanism of RC beams under close-in blast loading," *Eng. Fail. Anal.*, vol. 51, pp. 9-19, March 2015.

[15] E. Włodarczyk, "Mechanical impact of point explosion on the walls and ceiling of object," *Bulletin MUT*, vol. 39, no. 11, pp. 131-153, November 1980. (in Polish)

[16] V. R. Feldgun, Y. S. Karinski, D. Z. Yankelevsky, "A simplified model with lumped parameters for explosion venting simulation," *Int. J. Impact Eng.*, vol. 38, no. 12, pp. 964-975, December 2011.

[17] J. Siwiński, A. Stolarski, "Analysis of the internal explosion affecting building barriers," *Bulletin MUT*, vol. 64, no. 2, pp. 197-211, June 2015. (in Polish)

★★★